A Hybrid Quantum-Classical Framework for Solving Computational Fluid Dynamics and Nuclear Physics Equations using Quantum Singular Value Decomposition and Transformation

Devon Bontrager*, Kareem El-Araby*, Manu Chaudhary†, Alvir Nobel*,
Pruthviraj Sadhankar*, Shivansh Shrivas*, Trey Campbell*, Jacob Spry*, Naveed Mahmud‡,
Chao Lu§, Kalyan Gottiparthi§, Muralikrishnan Gopalakrishnan Meena§, Zain Karriem§, and Esam El-Araby*

*Department of Electrical Engineering and Computer Science (EECS), University of Kansas, Lawrence, KS, USA;
{devonlbontrager, kareem_el_araby, islam.alvir, pruthviraj.sadhankar, shivansh, trey.campbell, jacobspry, esam}@ku.edu
†Department of Electrical Engineering, Illinois State University, Normal, IL, USA; mchaud4@ilstu.edu
‡Department of EECS, Florida Institute of Technology, Melbourne, FL, USA; nmahmud@fit.edu
§Oak Ridge National Laboratory, Oak Ridge, TN, USA; {luc1, gottiparthik, gopalakrishm, karriemz}@ornl.gov

***Abstract*—Quantum computing offers a great promise to significantly reduce the computational cost of solving multidimensional partial differential equations (PDEs). However, existing quantum linear solvers, such as the Harrow–Hassidim–Lloyd (HHL) algorithm, exhibit limited scalability, prolonged execution times, and low accuracy. We propose a hybrid quantum-classical framework comprising two quantum PDE solvers based on quantum singular value decomposition (QSVD) and quantum singular value transformation (QSVT). The proposed methodology is validated on PDEs from computational fluid dynamics and nuclear engineering—potential flow past a 2D cylinder and a Joukowsky airfoil, and the neutron transport equation (NTE)—using noise-free and noisy simulators and hardware emulators from IBM-Quantum. The results demonstrate the feasibility of the proposed methods.**

***Index Terms*—Partial Differential Equations, Quantum Singular Value Decomposition, Quantum Singular Value Transformation**

I. Introduction and Motivation

The solution of partial differential equations (PDEs) is a fundamental computational challenge across science and engineering domains. Multidimensional PDEs are particularly difficult because the curse of dimensionality substantially increases computational cost [1]. These limitations have motivated investigation and development of quantum methods for solving PDEs [2]–[5]. Existing quantum PDE solvers however face several important limitations. PDE solvers based on the Harrow–Hassidim–Lloyd (HHL) algorithm attain logarithmic gate complexity only for sparse, well-conditioned, Hermitian matrices [13], whereas variational quantum algorithms (VQAs) for noisy intermediate-scale-quantum (NISQ) devices suffer from barren plateaus, high optimization costs, and limited accuracy [14]. To address these limitations, we propose a hybrid quantum-classical framework with two solvers based on quantum singular value decomposition (QSVD) and quantum singular value transformation (QSVT), validated on computational fluid dynamics (CFD) and nuclear engineering use cases.

II. Proposed Methodology and Case Studies

As illustrated in Fig. 1, the input PDE is discretized into a linear system $Au = b$ using the finite-difference method (FDM) [6] and re-balanced into $\tilde{A}\tilde{x} = \tilde{b}$ through iterative Ruiz Equilibration (REQ) [7], see (1), where the diagonal matrices D_r and D_c equilibrate the row and column norms of $\tilde{A}$.

$$\tilde{A} = D_r A D_c, \qquad \tilde{b} = D_r b, \qquad u = D_c\,\tilde{x} \tag{1}$$

A. QSVD Solver Workflow

During pre-processing, classical singular value decomposition (SVD) [8] factorizes the balanced operator as $\tilde{A} = W\Sigma V^\dagger$, followed by Polar Decomposition (PD) [9]. The input state is then prepared through classical-to-quantum (C2Q) encoding [15], [16], and the circuit is synthesized using column-by-column decomposition (CCD) [17]. Classical post-processing recovers the solution through denormalization and descaling, and the complete formulation is presented in [18], [19].

B. QSVT Solver Workflow

In the QSVT workflow [10], $\tilde{A}$ is embedded in the Hermitian dilation $H = \begin{bmatrix} 0 & \tilde{A} \\ \tilde{A}^\dagger & 0 \end{bmatrix}$, normalized as $\hat{H} = H/\alpha$ such that its spectrum lies in $[-1, 1]$, and $\tilde{b}$ is embedded as $|b_{\text{emb}}\rangle$. Matrix inversion is realized by approximating $1/x$ over its nonzero spectrum with an odd Chebyshev polynomial $P_d(x)$ of degree d, see (2).

$$P_d(\hat{H})\,|b_{\text{emb}}\rangle \approx \hat{H}^{-1}\,|b_{\text{emb}}\rangle. \tag{2}$$

The Chebyshev coefficients are converted into QSVT phases using the `pyqsp` package [11], [12], and the resulting circuit

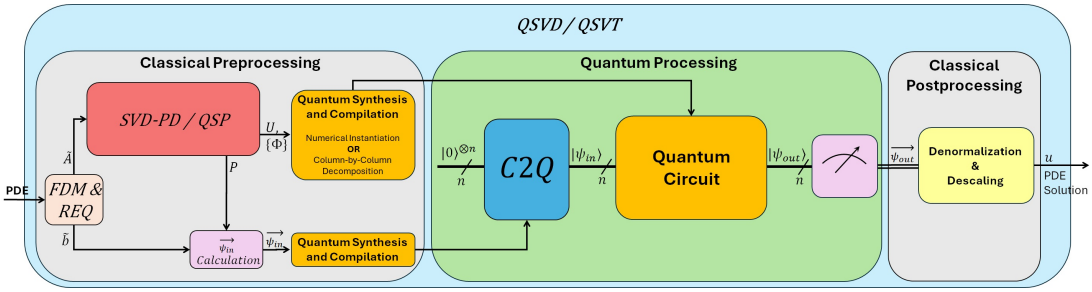


Fig. 1: Overview of the proposed QSVD/QSVT framework. The input PDE is discretized using FDM [6] and re-balanced using REQ [7]. QSVD pre-processing includes SVD [8] followed by Polar Decomposition (PD) [9]. QSVT [10] pre-processing involves Quantum Signal Processing (QSP) methods [11], [12], e.g., Block Encoding (BE) and Chebyshev Expansion (CE).

interleaves ancilla phase rotations with alternating block-encoding unitaries $U_{\hat{H}}$ and $U_{\hat{H}}^{\dagger}$ prior to CCD synthesis. Post-selecting the ancilla outcome $|0\rangle_a$ yields a state proportional to the scaled solution, and post-processing reverses the normalization and REQ to recover $u = D_c\tilde{x}$.

C. Case Studies

In CFD, incompressible, irrotational potential flow around a body is characterized by the stream function ψ, satisfying the Laplace equation $\nabla^2\psi = 0$ [20]. Three geometries are considered: a circular cylinder ($x^2 + y^2 \leq R^2$), a Joukowsky airfoil ($Z = \zeta + a^2/\zeta$) [20], and a Jayhawk logo [21].

The neutron transport equation (NTE) governs the angular neutron flux [22]. Assuming monoenergetic neutrons, steady state, linearly anisotropic scattering, and no external source, it reduces to the Helmholtz form

$$\nabla^2\phi(\mathbf{r}) + B_m^2\phi(\mathbf{r}) = 0, \tag{3}$$

where the material buckling $B_m^2 = (\nu\Sigma_f - \Sigma_a)/D$ and diffusion coefficient $D = 1/(3\Sigma_{tr})$ quantify net neutron production and absorption.

III. Experimental Setup

Experiments were conducted on a University of Kansas cluster node [23], on ORNL's Frontier supercomputer [24], [25], and on LBNL's Perlmutter supercomputer [26]. Experiments were conducted using noise-free and noisy simulators, and the hardware emulator (`FakeNighthawk`) of IBM-Qiskit [27].

A. Experimental Results

Tables I and II report the fidelity results of QSVD, QSVT, and an optimized QSVT variant (QSVT-Opt) for the three potential-flow geometries and the 2D NTE, along with their gate counts and circuit depths. QSVD results closely match the classical solution with high fidelity, while QSVT captures the overall trend with slight deviations because the underlying polynomial approximation of the inverse function results in a deep circuit with repeated chains of ancilla rotations and block-encoded unitaries. However, QSVT-Opt bypasses this repeated chain by pre-computing the circuit unitary followed by CCD, resulting in a circuit structure that is orders of magnitude more depth-optimized than QSVT and thereby achieving better fidelity. Since the circuits generated by QSVT are too deep for the emulator, they could not be run within practically reasonable execution times and the corresponding fidelity entries in Tables I and II are denoted as N/A.

TABLE I: 2D Potential Flow Results

Object	Solver	Fidelity			Gate Count		Circuit Depth	
		Statevector	AerSim	Emulator	AerSim	Emulator	AerSim	Emulator
Cylinder	QSVD	1.0	0.999999	0.808936	174	327,973	161	195,892
Cylinder	QSVT	0.999997	0.999962	N/A	1,202	4,825,710,458	1,201	2,974,079,518
Cylinder	QSVT-Opt	0.999997	0.999952	0.836766	1,416,904	14,831,400	1,416,903	9,205,237
Airfoil	QSVD	1.0	0.999999	0.805838	263	330,933	250	197,763
Airfoil	QSVT	0.999992	0.999953	N/A	1,202	4,817,703,210	1,201	2,950,608,624
Airfoil	QSVT-Opt	0.999992	0.999954	0.884381	1,416,904	14,849,910	1,416,903	9,224,946
Jayhawk	QSVD	1.0	0.999999	0.671472	263	328,263	250	195,248
Jayhawk	QSVT	0.999997	0.999942	N/A	1,202	4,818,219,250	1,201	2,950,538,026
Jayhawk	QSVT-Opt	0.999997	0.999950	0.852658	1,416,904	14,852,044	1,416,903	9,228,859

Note: N/A indicates incomplete runs due to long execution time.

TABLE II: 2D Neutron Transport Equation Results

Object	Solver	Fidelity			Gate Count		Circuit Depth	
		Statevector	AerSim	Emulator	AerSim	Emulator	AerSim	Emulator
2D NTE	QSVD	1.0	0.999999	0.735440	394	171,442	380	105,288
2D NTE	QSVT	0.993105	0.992948	N/A	1,202	4,796,216,506	1,201	2,935,190,088
2D NTE	QSVT-Opt	0.993105	0.993098	0.732078	1,416,904	14,858,729	1,416,903	9,231,191

Note: N/A indicates incomplete runs due to long execution time.

IV. Conclusions and Future Work

This work presented a hybrid quantum-classical framework for solving PDEs using QSVD- and QSVT-based solvers. Experimental results demonstrate high-fidelity solutions in noisy simulation environments, alongside realistic gate counts and circuit depths from hardware emulation. Future work will focus on optimizing QSVT circuits for quantum-hardware deployment.

Acknowledgment

This research used resources of the Oak Ridge Leadership Computing Facility at the Oak Ridge National Laboratory, which is supported by the Advanced Scientific Computing Research programs in the Office of Science of the U.S. Department of Energy under Contract No. DE-AC05-00OR22725. This research also used resources of the National Energy Research Scientific Computing Center (NERSC), a Department of Energy Office of Science User Facility under Contract DE-AC02-05CH11231.

REFERENCES

[1] A. Cohen and R. DeVore, "Approximation of high-dimensional parametric PDEs," *Acta Numerica*, vol. 24, pp. 1–159, 2015.

[2] A. Di Meglio, K. Jansen, I. Tavernelli, C. Alexandrou, S. Arunachalam, C. W. Bauer, K. Borras, S. Carrazza, A. Crippa, V. Croft *et al.*, "Quantum computing for high-energy physics: state of the art and challenges," *PRX Quantum*, vol. 5, no. 3, p. 037001, 2024.

[3] W. Deng, J. Wang, A. Guo, and H. Zhao, "Quantum differential evolutionary algorithm with quantum-adaptive mutation strategy and population state evaluation framework for high-dimensional problems," *Information Sciences*, vol. 676, p. 120787, 2024.

[4] A. M. Childs, J.-P. Liu, and A. Ostrander, "High-precision quantum algorithms for partial differential equations," *Quantum*, vol. 5, p. 574, 2021.

[5] J.-P. Liu, H. O. Kolden, H. K. Krovi, N. F. Loureiro, K. Trivisa, and A. M. Childs, "Efficient quantum algorithm for dissipative nonlinear differential equations," *Proceedings of the National Academy of Sciences*, vol. 118, no. 35, p. e2026805118, 2021.

[6] J. R. Nagel, "Solving the generalized Poisson equation using the finite-difference method (FDM)," Lecture Notes, Department of Electrical and Computer Engineering, University of Utah, 2011.

[7] D. Ruiz, "A scaling algorithm to equilibrate both rows and columns norms in matrices," Rutherford Appleton Laboratory, Oxon, UK, Tech. Rep. RAL-TR-2001-034, 2001.

[8] G. W. Stewart, "On the early history of the singular value decomposition," *SIAM Review*, vol. 35, no. 4, pp. 551–566, 1993.

[9] G. Buffington, "Polar decomposition of a matrix," Advanced Linear Algebra (Math 420), 2014.

[10] A. Gilyén, Y. Su, G. H. Low, and N. Wiebe, "Quantum singular value transformation and beyond: exponential improvements for quantum matrix arithmetics," in *Proceedings of the 51st Annual ACM SIGACT Symposium on Theory of Computing*, 2019, pp. 193–204.

[11] Z. M. Rossi, J. L. Ceroni, and I. L. Chuang, "Modular quantum signal processing in many variables," arXiv preprint arXiv:2309.16665, 2023.

[12] PennyLane Development Team, "Intro to QSVT: Transforming matrices encoded in matrices," 2024, available: https://pennylane.ai/qml/demos/tutorial_intro_qsvt. Last Accessed: July 2026.

[13] A. W. Harrow, A. Hassidim, and S. Lloyd, "Quantum algorithm for linear systems of equations," *Physical Review Letters*, vol. 103, no. 15, p. 150502, 2009.

[14] A. J. Pool, A. D. Somoza, M. Lubasch, and B. Horstmann, "Solving partial differential equations using a quantum computer," in *2022 IEEE International Conference on Quantum Computing and Engineering (QCE)*. IEEE, 2022, pp. 864–866.

[15] E. El-Araby, N. Mahmud, M.-J. Jeng, A. MacGillivray, M. Chaudhary, M. A. I. Nobel, S. I. U. Islam, D. Levy, D. Kneidel, M. R. Watson, J. G. Bauer, and A. E. Riachi, "Towards complete and scalable emulation of quantum algorithms on high-performance reconfigurable computers," *IEEE Transactions on Computers*, vol. 72, no. 8, pp. 2350–2364, 2023.

[16] K. Ghosh, "Encoding classical data into a quantum computer," arXiv preprint arXiv:2107.09155, 2021.

[17] R. Iten, R. Colbeck, I. Kukuljan, J. Home, and M. Christandl, "Quantum circuits for isometries," *Physical Review A*, vol. 93, no. 3, p. 032318, 2016.

[18] M. Chaudhary, I. Islam, D. Levy, A. Nobel, D. Kneidel, V. Jha, and E. El-Araby, "An efficient quantum solver for multidimensional partial differential equations," in *International Conference on Emergent Quantum Technologies (ICEQT 2024)*, 2024.

[19] M. Chaudhary, K. El-Araby, A. Nobel, I. Islam, M. Singh, S. Ogundele, K. Egan, S. Thomas, V. Vordtriede, D. Bontrager, S. Kim, and E. El-Araby, "A practical quantum solver for multidimensional partial differential equations," in *Proceedings of the SC'25 Workshops of the International Conference for High Performance Computing, Networking, Storage and Analysis*, 2025, pp. 1916–1925.

[20] J. D. Anderson, *Fundamentals of Aerodynamics*, 6th ed. New York, NY, USA: McGraw-Hill Education, 2016.

[21] Brand Center, University of Kansas, "Jayhawk Images," 2026, available: https://brand.ku.edu/. Last Accessed: July 2026.

[22] J. R. Lamarsh and A. J. Baratta, *Introduction to Nuclear Engineering*, 3rd ed. Upper Saddle River, NJ: Prentice Hall, 2001.

[23] University of Kansas Center for Research Computing, "Systems and Services," 2026, available: https://crc.ku.edu/systems-services. Last Accessed: July 2026.

[24] Oak Ridge Leadership Computing Facility, "Frontier User Guide," 2026, available: https://docs.olcf.ornl.gov/systems/frontier_user_guide.html. Last Accessed: July 2026.

[25] S. Atchley *et al.*, "Frontier: Exploring exascale," in *Proc. Int. Conf. High Performance Computing, Networking, Storage and Analysis (SC '23)*, 2023.

[26] NERSC, "Perlmutter architecture," https://docs.nersc.gov/systems/perlmutter/architecture/, last Accessed: July 2026.

[27] IBM Quantum, "Qiskit: An open-source framework for quantum computing," 2026, available: https://www.ibm.com/quantum/qiskit. Last Accessed: July 2026.